Tetrahedron 75 (2019) 129–136

Contents lists available at ScienceDirect

Tetrahedron

journal homepage: www.elsevier.com/locate/tet

Radical-clock α-halo-esters as mechanistic probes for bisphosphine iron-catalyzed cross-coupling reactions

Lei Liu, Wes Lee, Jun Zhou [1], Surjo Bandyopadhyay, Osvaldo Gutierrez*

Department of Chemistry and Biochemistry, University of Maryland, College Park, MD, 20742, United States

ARTICLE INFO

Article history:
Received 30 August 2018
Received in revised form
19 November 2018
Accepted 21 November 2018
Available online 1 December 2018

Keywords:
Tandem cyclization-arylation reactions
Bisphosphine-iron
Cross-coupling reactions
Mechanisms
DFT

ABSTRACT

The mechanism of chiral bisphosphine iron-catalyzed C(sp^2)-C(sp^3) cross-coupling reactions has been studied via the synthesis of novel radical-clock α-halo-esters and quantum mechanical calculations. These results provide insights into the role of the substrate (halogen and substituents) in competing *in-cage* and *out-of-cage* arylation pathways and provide a basis for the future rational design of novel tandem cyclization-arylation reactions using bisphosphine-iron as catalysts.

1. Introduction

Cross-coupling reactions remain the method of choice for the construction of C–C bonds. In this vein, significant progress has been accomplished using palladium and, more recently, nickel as transition metal catalysts to promote cross-coupling reactions using a wide range of electrophiles and nucleophiles [1]. Recently, iron has resurfaced as a cheaper, less toxic, and more Earth-abundant transition metal alternative to promote C–C cross-coupling reactions [2]. In particular, bisphosphine-iron systems have been reported by Nakamura [3], Bedford [4], Chai [5], Fürstner [6], and Baran [7] to promote cross-coupling reactions using alkyl halides and redox active esters as radical precursors. However, our understanding of the mechanisms of these transformations is limited. Without a doubt, further fundamental mechanistic studies are critical to advance the field [8]. For instance, aside from the seminal report by Nakamura and co-workers using α-halo-esters and aryl Grignard reagents (Scheme 1A) [9], methods for iron-catalyzed *asymmetric* cross-couplings are nonexistent [10]. On the other hand, many transition metal-catalyzed (e.g., nickel and palladium) asymmetric cross-coupling reactions have been reported [11]. Previously, Nakamura-Morokuma [12] and we [13] used quantum mechanical calculations to investigate the mechanism of chiral bisphosphine iron-catalyzed C(sp^2)-C(sp^3) cross-coupling reactions. Our studies revealed similar Fe(I)/Fe(II)/Fe(III) catalytic cycles for this transformation, Scheme 1B, and Scheme 1C, respectively. Although evidence for the participation of alkyl radicals is strong, the factors that control alkyl radical (e.g., *in-cage* or *out-of-cage*) arylation are not known. Previously, Nakamura used **1a** and **1b** as mechanistic probes in the asymmetric iron-catalyzed cross-coupling reaction using chiral bisphosphine ligand **BenzP***(Scheme 2) [9]. Under standard conditions (e.g., slow addition of aryl Grignard), α-chloro ester **1a** formed a mixture of the *acyclic* (*enantioenriched*) and *cyclic* (*racemic*) cross-coupled products **2a** and **3a** in low yields, 12% and 40%, respectively (Scheme 2). Moreover, a first-order relationship between the ratio of *acyclic*/*cyclic* cross-coupled product (**2a**/**3a**) and catalyst concentration supported a competing *out-of-cage* radical pathway in which *apparent radical lifetime is inversely proportional to the degree of radical clock rearrangement* [14]. Substrate **1b** that bear pendant olefin with *Z* stereochemistry also provided a mixture of the corresponding *acyclic* (*enantioenriched*) and *cyclic* (*racemic*) cross-coupled products, **2b** and **3b** respectively (Scheme 2, red). Moreover, the observation that both *acyclic* cross-coupled product **2b** and *recovered starting material* **1b** retained *Z* stereochemistry suggests that after cyclization occurs the process is irreversible (Scheme 2). Herein, we use a series of sensitive α-halo esters as

* Corresponding author.
E-mail address: ogs@umd.edu (O. Gutierrez).
[1] Current location: School of Chemistry and Biological Engineering, Changsha University of Science & Technology, Changsha, Hunan, 410114, China.

https://doi.org/10.1016/j.tet.2018.11.043
0040-4020/

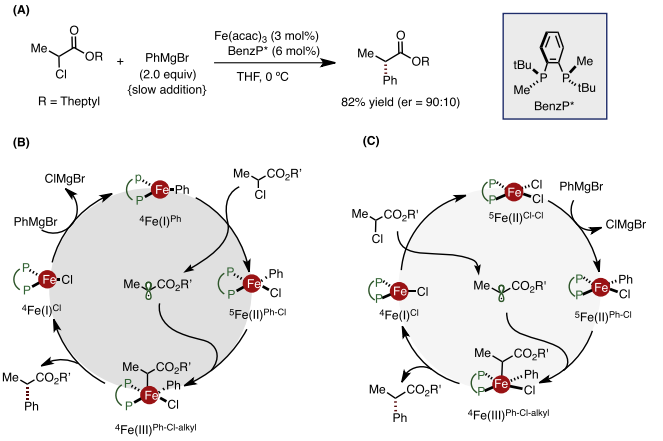

Scheme 1.

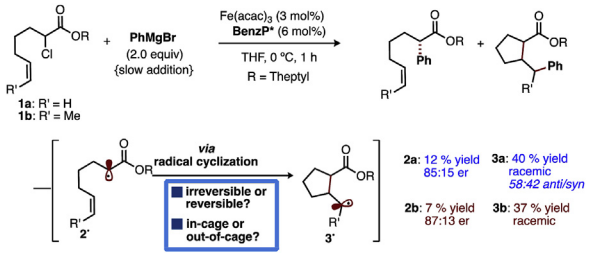

Scheme 2.

mechanistic probes together with quantum mechanical calculations to elucidate at the fate of the alkyls radicals in bisphosphine-iron catalyzed cross-coupling reactions. Implications for the rational design of iron-catalyzed enantioselective tandem radical cyclization-arylation reaction are discussed.

2. Results/discussion

We began our study by computing the energetics for radical cyclization of the alkyl radicals **2a•** and **2b•**, presumably formed directly from probes **1a** and **1b**, respectively, via halogen abstraction by iron(I) (Scheme 1B/**C**). All energies discussed are for singlet spin states (for non-transition metals) were performed at the (U) DLPNO-CCSD(T)/def2-TZVPP//UB3LYP/6-31G(d) level of theory. DFT optimizations were performed using Guassian09 [15], and (U) DLPNO-CCSD(T) single point energy calculations were performed using ORCA [16]. For simplicity, primarily (U)DLPNO-CCSD(T) energies will be discussed. As shown in Fig. 1, for the unsubstituted probe **1a**, the lowest energy barrier for radical cyclization of **2a•** is 5.7 kcal/mol (via **3a• -TS-*anti***), which will lead to the formation of 3**a• -*anti*** (downhill in energy by 10.9 kcal/mol). This barrier is in excellent agreement with the experimental activation barrier ~6 kcal/mol (rate constant $k \sim 10^5$ s^{-1}) for the analogous α-radical (R = Et) and allows us to calibrate our computational methods [17]. Not surprisingly, the cyclization barrier for the methyl-substituted *Z* olefin **2b•** (from probe **1b**) is significantly lower (~2 kcal/mol; via **3b• -TS-*syn***) and more exergonic (12.1 kcal/mol) reflecting the additional stability provided by the methyl to the incipient cyclized radical. Notably, the lowest energy barrier to undergo *reversible* cyclization (i.e., from **3b•-*syn*** to **2b•**) is only 16.0 kcal/mol. Given both *acyclic* cross-coupled product **2b** and recovered starting material **1b** retained *Z* stereochemistry, these computational results suggest that 1) the barrier for *direct (in-cage) arylation* must be in

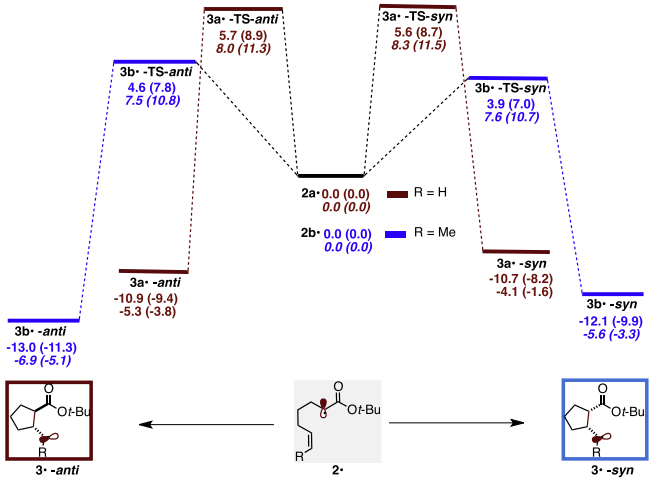

Fig. 1. Energetics for radical cyclization of **1a** (red) and **1b** (blue) calculated at the (U) DLPNO-CCSD(T)/def2-TZVPP//UB3LYP/6-31G(d) and UB3LYP/6-31G(d) [italics] level of theory. Enthalpies and free energies are in kcal/mol.

the 4–5 kcal/mol range (i.e., *relatively similar in magnitude as radical cyclization*); and 2) downstream arylation (*in-cage or out-of-cage*) of the cyclized radical must be faster than the reverse ring-opening barrier (less than ca. 17 kcal/mol).

We hypothesize that a more sensitive radical clock substrate could lead to the exclusive formation of cyclized product(s) by outcompeting the *direct* (*in-cage*) arylation of acyclic alkyl radical and, in turn, define the upper limit for *in-cage* arylation in these systems. Newcomb and co-workers have measured the rate constants for substituted alkyl radicals to undergo 5-*exo* cyclizations in the range of $k = 10^5$–10^8 s^{-1} (at room temperature) [17]. These studies also show that the rates for radical cyclization are faster for substrates that bear groups that stabilize the incipient cyclized radicals. For instance, the rate for *5-exo* cyclization of ethyl hept-6-enoate radical is 1.4×10^5 s^{-1} while that of the corresponding radical ethyl 1,1-diphenyl-hept-6-enoate is more than two orders of magnitude faster (i.e., $k = 5 \times 10^7$ s^{-1}). As such, we synthesized a series of α-alkyl esters with pendant esters (**7a-c**; Scheme 3A) using a short and highly versatile synthetic route (Scheme 3B). We chose these substrates due to ease of synthesis, presumed barrier lowering of the *5-exo* radical cyclization (**8•** to **9•**) by the ester moiety via stabilization of the incipient radical, and potential for pendant ester group to induce asymmetry in the tandem cyclization-arylation reaction [18].

As shown in Scheme 3B, we synthesized the desired α-halo esters in 3–4 steps from commercially starting materials in modest to good yields. To the best of our knowledge, the effect of pendant ester moiety on *5-exo* radical cyclizations has not been determined. Therefore, we computed the energetics for *5-exo* radical cyclization starting from **8•** (presumably formed directly from halogen abstraction of α-alkyl esters **7a-c**) to explore the effect of the ester group. As shown in Scheme 3C, the barrier for *5-exo* radical cyclization of ester-substituted **8•** is much lower (~2–4 kcal/mol) in energy than of previous used radical probes **2a•** and **2b•** (Fig. 1) [19] and also 4–7 kcal/mol more exothermic. We attribute the lower barrier and larger exothermicity to the resonance stabilization of the incipient radical by ester group. These computations suggest that the *relative rate of 5-exo radical cyclization of **8•** should be at least 100-times faster than direct (in-cage) arylation* leading to the corresponding cyclized radicals [20]. Moreover, since the barrier for cyclization of **8•** is much lower than previously explored systems (Fig. 1), we hypothesize that **8•** will quickly cyclize (to **9•**) rather

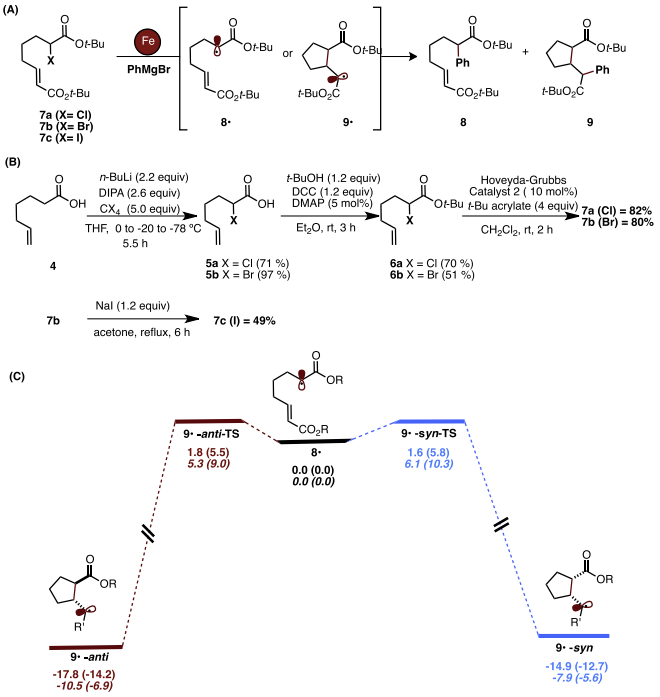

Scheme 3. Energetics for radical cyclization of **8•** (R = *tert*-butyl) calculated at the (U) DLPNO-CCSD(T)/def2-TZVPP//UB3LYP/6-31G(d) and UB3LYP/6-31G(d) [italics] level of theory. Enthalpies and free energies are in kcal/mol.

than undergoing direct (in-cage) arylation. Ultimately, cyclic radical **9•** will undergo arylation to form **9**. Alternatively, if *acyclic* product **8** is observed, it will suggest that subsequent C–C bond formation of the cyclized radicals is much higher in energy than the *combined* energy penalty to undergo *reverse* ring-opening (16–19) followed by C–C bond formation of *acyclic radical* **8•**.

With mechanistic probes in hand, we subjected **7a-c** to standard iron-catalyzed cross-coupling conditions (Table 1). In agreement low barrier for radical cyclization of **8•** (Scheme 3C), we did not observe the formation of *acyclic* cross-coupled product **8**, presumably from direct (in-cage) arylation. Instead, we found tandem radical cyclization-arylation product **9** as a mixture of four diastereomers, albeit in low (28%) yield (entry 1). Nonetheless, these results indicate that the radical cyclization outcompetes *in-cage* arylation of **8•** and sets the upper limit for the rate of direct arylation at **8•** at ~10^5 s^{-1}. Notably, we also found 30% yield of the cyclized protonated product **10** (entry 1). Control experiments without bisphosphine ligand (entry 2) show similar yields of **10** but no formation of the cyclic cross-coupled product **8** [21]. Overall, these results indicate that formation of cyclized protonated product **10** is likely a result of ferrate chemistry (e.g., dehalogenation, conjugate addition, and protonation) although the mechanism is not well elucidated [22].

Previously, Nakamura reported that chiral ligand **BenzP*** and **QuinoxP*** deliver nearly identical enantioselectivities albeit slightly lower yields [9]. Thus, we also explored the reactivity and selectivity of this ligand with mechanistic probes **7a-c**. To our surprise, changing the ligand from **BenzP*** to **QuinoxP*** completely shut down the tandem cyclization-arylation pathway while still forming (ferrate chemistry) product **10** in 62% yield (entry 3). Notably, we were able to turn back on the reactivity of the tandem cyclization-arylation pathway by switching the substrate from α–chloro **7a** to α–bromo ester **7b** (entry 4), which resulted in the formation of **9** albeit lower yields than the α–chloro **7a** and **BenzP*** ligand combination. Moreover, as with α-chloro esters, control experiment (entry 5) revealed that the bisphosphine ligand is crucial to promote tandem cyclization-arylation reaction with α–bromo **7b** [23]. Notably, iodo ester **7c** provided both **9** and **10** in 38% and 55% yield, respectively (entry 6). However, the observed reactivity with iodo probe (i.e., the formation of **9** and **10**) is likely a result of ligand-less (e.g., ferrate) chemistry as evident from nearly identical results in the absence of bisphosphine ligand (entry 7) [24,25]. Overall, these results suggest that the reactivity of the tandem cyclization-arylation is highly dependent on subtle

Table 1
Mechanistic experiments of bisphosphine iron-catalyzed cross-coupling reactions.[a]

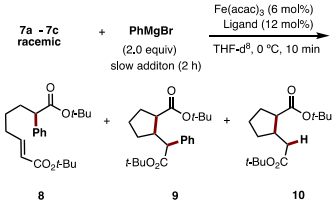

Entry	7	ligand	yield[b] 8 (%)	yield[b] 9 (%)	yield[b] 10 (%)	conversion[b] (%)
1	**7a**	BenzP*	NA	28 (1:4:1.5:1.5)	30 (1.5:1)	85
2	**7a**	NA	NA	NA	25 (1.5:1)	63
3	**7a**	QuinoxP*	NA	NA	62 (1.4:1)	92
4	**7b**	QuinoxP*	NA	16 (1:4:1.5:1.5)	52 (1.6:1)	100
5	**7b**	NA	NA	NA	41 (1.4:1)	83
6	**7c**	QuinoxP*	NA	38 (1:2:1:1)	55 (1.5:1)	100
7	**7c**	NA	NA	34 (1:6.7:2:1.7)	56 (1.5:1)	90

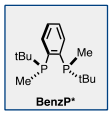

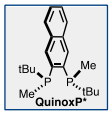

[a] Conditions: reactions were performed using 0.1 mmol of α-halo ester, 6 mol % of $Fe(acac)_3$, 12 mol % of ligand, and 2.0 equiv of PhMgBr in solvent (1.0 M) at 0 °C for 10min. PhMgBr was added slowly over the course of 2.0 h via syringe pump.
[b] Determined by crude ^1H NMR with dibromomethane as internal standard.

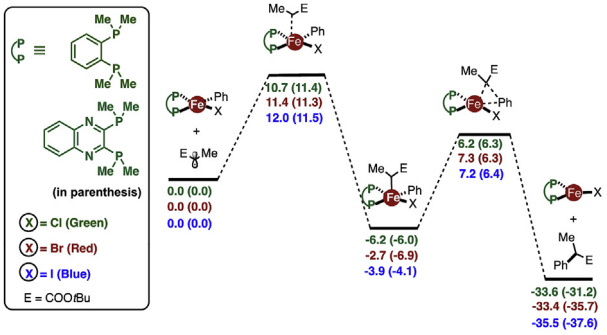

Fig. 2. Halogen and ligand effect on the iron-catalyzed C-C bond formation step via quartet spin state. Free energies are in kcal/mol. (U)PBEPBE/6-311 + G(d,p)-SDD(Fe,Cl,Br,I)-THF(SMD)//(U)B3LYP/6-31G(d)-LANL2DZ(Cl,Br,I).

changes to the bisphosphine ligand and nature of alkyl halide. Notably, model calculations (Fig. 2) revealed no effect of the ligand electronics (**BenzP*** vs. **QuinoxP***) or halogen on the arylation step (i.e., radical addition or reductive elimination) [26]. These results are consistent with the formation of α-alkyl radicals (i.e., halogen abstraction) as the rate-determining step and more sensitive to the nature of the ligand and the alkyl halide in the tandem cyclization-arylation reaction (*vide infra*). Calculations are underway to explore the effect of ligand and halide in the formation of alkyl radicals and determining the barriers for C–C bond formation using the full cyclized systems.

We envisioned probing the effect of reversibility 5-*exo* cyclization of iron-catalyzed cross-coupling reactions using **13** as a mechanistic probe (Scheme 4). Specifically, we hypothesized that radical cyclization should follow ring-opening of the cyclopropyl group to form the thermodynamically more stable *cyclic*-ring-opened alkyl radical thus increasing both the thermodynamic drive and barrier for *reverse* reaction.

Using a similar synthetic route (*vide supra*), we synthesized the desired α-chloro ester with pendant vinyl cyclopropyl group mechanistic probe **13** as an inseparable 3.5: 1 (*Z*: *E*) mixture (Scheme 4A). As shown in Scheme 4B, *the reaction with **13** formed nearly exclusive cascade cyclization-ring-opening-arylation products (85% combined yield)!* Specifically, we found the formation of the corresponding *anti* cyclic/ring-opened products **15-*anti-E*** in 60% yield and 25% yield of **15-*anti-Z***. Notably, this result provides further support for the participation of *cyclic alkyl radicals before (out-of-cage) arylation*. The lack of *acyclic* cross-coupled product **14** implies that the direct (*in-cage*) arylation is slower than the cascade radical cyclization, ring-opening, arylation process (*vide infra*).

To gain insights into the reversibility of the radical cyclization in this system, we turned to quantum mechanical calculations. As shown in Fig. 3, the barrier for 5-*exo* radical cyclization is only ca. 4 kcal/mol and exothermic by ca. 13–15 kcal/mol leading to both *syn*- and *anti*-cyclic alkyl radicals **15•*Z-anti*** and **15•*Z-syn***. Further, although radical **13•*Z*** (from probe **13**) is analogous to radical **2b•**, the barrier for cyclization of **13•** is slightly lower (0.2 kcal/mol) than radical cyclization of **2b•** [27]. Notably, **1b** formed direct arylation product **2b** (from **2b•**) while no direct cross-coupled product was observed with **13** (from **13•*Z***). This result implies that by lowering the barrier for radical cyclization, it is possible to outcompete (and even shut down) the direct (in-cage) arylation pathway.

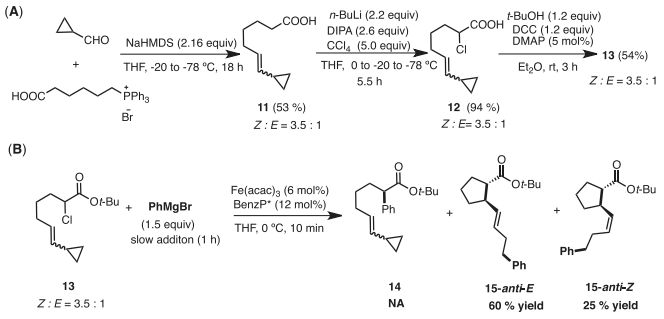

Scheme 4.

Finally, cyclopropyl ring-opening will lead to the much more thermodynamically stable ring-opened products **15• -*anti-E/Z*** and **15• -*syn-E/Z*** (either directly from **15•*Z-anti*** and **15•*Z-syn*** or from rotation to **15•E-*anti*** and **15•E-*syn*** followed by ring-opening). Importantly, the barriers for the reverse reaction (ca. 21 kcal/mol) to get back to **13•** are insurmountable at experimental conditions and therefore, contrary to previous probes, convincingly irreversible (not under a Curtin-Hammett scenario). Although, **15• -*anti-E*** and **15• -*anti-Z*** can interconvert (under Curtin-Hammett scenario) via the 3-member ring closing/ring opening. Experimentally, we observed the 5-member *anti* as the major products (up to 85% yield) and only observed minor amounts of the *syn* 5-member cyclized products. This observation is more consistent with the B3LYP computations, which predict a ca. 1 kcal/mol lower barrier for the *anti*-cyclization (**15•-Z-anti-TS**) in comparison to the *syn*-cyclization. Overall, the observed product distributions can be rationalized based on the preference for the irreversible *anti* 5-member cyclization-ring-opening and subsequent relative barriers for the competing C–C bond formation of the cyclic/ring-opened alkyl radicals **15• -*anti-E/Z***.

Through the synthesis of new radical clock mechanistic probes and quantum mechanical calculations, we have bracketed the rate for alkyl radical arylation to ca. 5 kcal/mol at the (U)DLPNO-CCSD(T)/def2-TZVPP//UB3LYP/6-31G(d) level of theory. Taken together, we propose the working hypothesis presented in Fig. 4 in which competing *in-cage* and *out-of-cage* arylation pathways are operative. (A) For *short-lived* alkyl radicals [e.g., at this level of theory, when the barrier for radical cyclization is higher than 5 kcal/mol], direct (in-cage) arylation of alkyl radical **A•** will form a*cyclic* cross-coupled product **A** with apparent "*retention*" of stereochemistry [probe **1a** and **1b**]. Nonetheless, although the strength of the cage (e.g., local viscosity of solvent) is likely to play a significant role in the efficiency of direct arylation (i.e., from rapid, radical rebound) [28], the rate of diffusion should be much faster ($k = \times 10^9\ s^{-1}$) [29] and thus some leakage of alkyl radicals will inherently occur. For alkyl radicals without pendant olefins, cross-coupled products from competing in-cage (direct) *and* out-of-cage arylation will form the same acyclic arylated product (e.g., Scheme 1A). The competition between in-cage and out-of-cage is consistent with the first-order relationship between the ratio of acyclic/cyclic cross-coupled products and catalyst loading. (B) As the barrier for radical cyclization lowers (e.g., by tuning the properties of the pendant olefin) a higher concentration of acyclic radical **2•** will (in-cage) cyclize to (*more thermodynamically stable*) *cyclic* radical thus increasing the apparent lifetime of the radical [probe **8**]. As such, this persistent *cyclic* alkyl radical [30] can escape the solvent cage and capture the transient aryl iron species to undergo C–C bond formation. Given the structural similarities between **A•** and **B•**, we can assume that the relative barriers for C–C bond formation are similar. Therefore, combined with the fact that the cyclic radical is thermodynamically lower in energy than acyclic radical, **B•** will undergo, preferentially faster, *out-of-cage* radical arylation leading to the formation of cyclic cross-coupled product **B**. As the thermodynamic drive for cyclic radicals increases (non-Curtin-Hammett scenario) to prevent reversible cyclization (e.g., with pendant cyclopropyl group) only cyclic cross-coupled products will form from arylation of

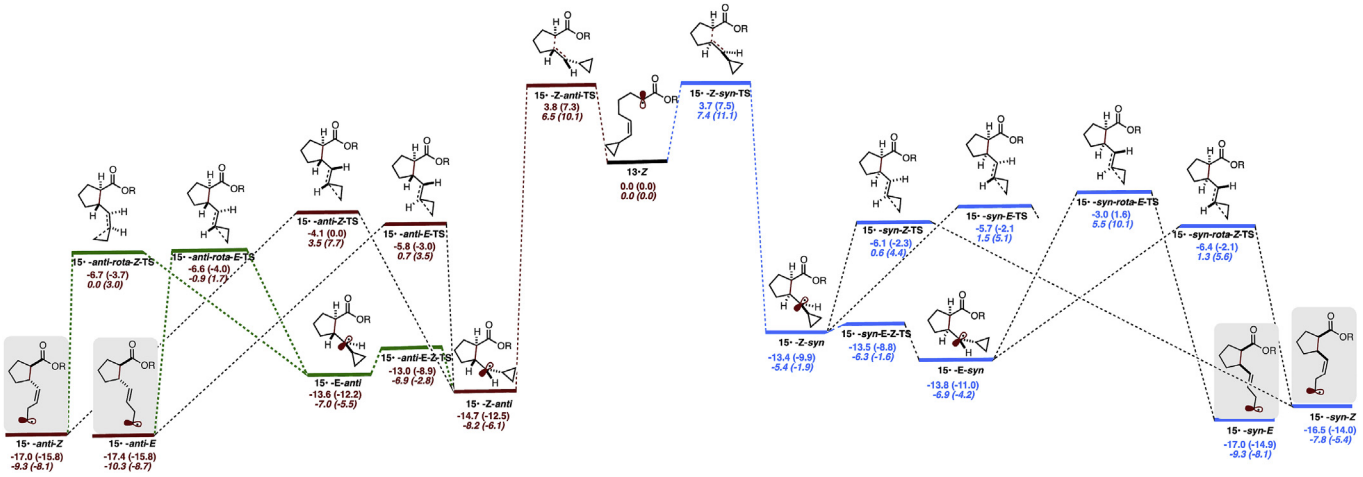

Fig. 3. Energetics for radical cyclization of **13•** (R = CO_2*t*Bu) calculated at the (U)DLPNO-CCSD(T)/def2-TZVPP//UB3LYP/6-31G(d) level of theory and UB3LYP/6-31G(d) [italics]. Enthalpies and free energies (in parenthesis) are in kcal/mol.

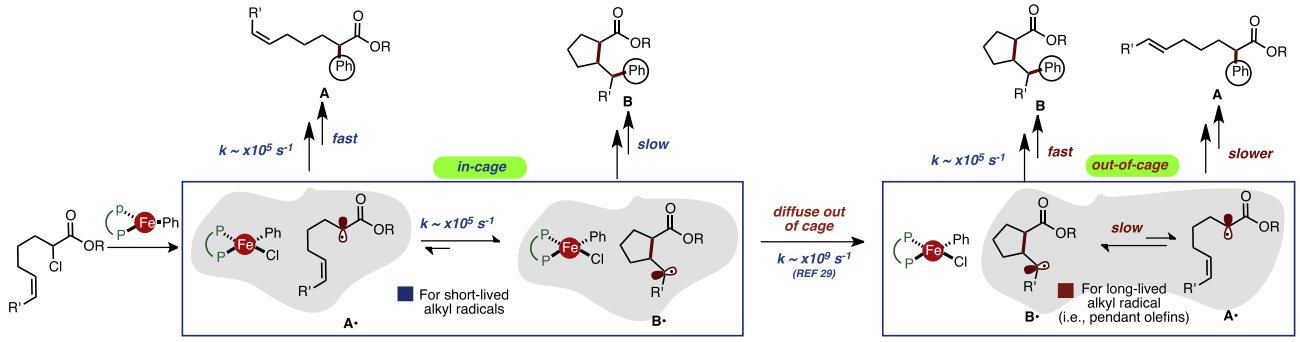

Fig. 4. Working hypothesis.

downstream alkyl radicals [probe **13**].

3. Conclusion

The mechanism of chiral bisphosphine iron-catalyzed C(sp^2)-C(sp^3) cross-coupling reactions has been studied via the synthesis of novel radical-clock mechanistic probes and DLPNO-CCSD(T) calculations. From a broader perspective, these results indicate that, in principle, alkyl halides can participate in selective tandem cyclization-arylation reactions, which remain a challenge in iron catalysis. We are currently exploring the scope of this transformation and the development of enantioselective tandem-cyclization/arylation reactions and will report in due course.

4. Experimental section

4.1. General

Unless otherwise stated, all non-aqueous reactions were carried out under an atmosphere of dry nitrogen in oven- (150 °C) or flame-dried glassware. When necessary, solvents and reagents were dried prior to use. Dichloromethane was distilled from CaH_2. Tetrahydrofuran was dried by passage through activated alumina in Inert's PureSolv PS-MD-3 solvent purification system. All work-up and purification procedures used reagent grade solvents purchased from VRW, Sigma-Aldrich, or Fisher. Organometallic reagents were purchased from Sigma-Aldrich. Analytical thin layer chromatography (TLC) was performed on Silicycle 250 μm silica-gel F-254 plates. Column chromatography was performed on pre-packed silica-gel cartridges (SNAP Ultra; Biotage). Purification via flash column chromatography was performed on silica gel 60 (230–400 mesh ASTM). ^{1}H NMR and ^{13}C NMR spectra were recorded on Bruker AV (400 MHz), Bruker DRX (500 MHz) or Bruker AV-III (600 MHz) NMR spectrometer. Chemical shifts (δ) are reported in parts per million (ppm) relative to the internal residual solvent resonance peak δ 7.26 ($CDCl_3$) and δ 0.00 (TMS) for ^{1}H and δ 77.16 ($CDCl_3$) and δ 0.00 (TMS) for ^{13}C. Data are reported as follows: chemical shift, multiplicity (s = singlet, d = doublet, t = triplet, q = quartet, b = broad singlet, m = multiplet, dd = doublet of doublets, dt = doublet of triplets, ddt = doublet of doublet of triplets), coupling constants (*J*) are reported in Hertz (Hz), and number of protons. High Resolution Mass (HRMS) spectra using Electrospray Ionization (ESI) mode was obtained using a JEOL AccuTOF-CS.

4.1.1. General procedure for the synthesis of α-halo esters **6a**, **6b** and **13**

To a stirred solution of *N,N′*-dicyclohexylcarbodiimide (DCC) (1.24 g, 6 mmol) in diethyl ether (15 mL) was added α-halo hept-6-enoic acid [9,31] (5 mmol) at room temperature. Then a mixed solution of the *tert*-butanol (6 mmol) and 4-dimethylaminopyridine (DMAP) (36.7 mg, 0.3 mmol) in diethyl ether (5 mL) was added via syringe dropwise. Upon addition of the mixed solution of *tert*-butanol and DMAP, a precipitate began to form. After the addition was complete, the reaction mixture was maintained for 3 h at the same temperature, then diluted with

hexanes (20 mL). The resulting mixture was filtered through a celite pad and the filtrate was concentrated under reduced pressure. The crude product was purified by silica gel chromatography to yield the α-halo esters (hexane:EtOAc = 30:1).

4.1.2. General procedure for the synthesis of di-tert-butyl (E)-7-halooct-2-enedioate **7a-c**

To a solution of 2-chlorohept-7-enoate ester **6a** or 2-bromohept-7-enoate este **6b** (2 mmol) in dichloromethane (20 mL) was added the *tert*-butyl acrylate (8 mmol) followed by the catalyst Hoveyda-Grubbs catalyst 2nd generation (0.2 mmol). After the addition was complete, the reaction mixture was maintained for 2 h at the room temperature. The resulting mixture was filtered through a short pad of silica gel. The solvent was removed in *vacuo*, and the residue was purified by silica gel chromatography (Hexane:EtOAc = 20:1), affording the desired product **7a** and **7b** [32].

To a flask equipped with a stir bar and reflux condenser was added NaI (0.44 g, 2.9 mmol) and di-*tert*-butyl (*E*)-7-bromooct-2-enedioate **7b** (0.87 g, 2.4 mmol) followed by acetone (2.4 mL). The flask was sealed and purged with nitrogen and allowed to reflux for 6.0 h. The mixture was allowed to cool to room temperature and H_2O (5 mL) was added to dissolve the resulting white precipitate. The layers were separated and the aqueous layer was washed with (5 mL × 3) diethyl ether. The combined organic phase was washed with a 10% solution of aqueous $Na_2S_2O_3$ (5 mL). The organic layer was then dried over $MgSO_4$ and concentrated in *vacuo*. The resulting residue was purified through silica gel chromatography (hexane:EtOAc = 20:1), affording the desired product **7c**.The synthesis was not optimized [33].

4.1.3. General procedure of iron-catalyzed tandem cyclization-arylation reactions

To a stirred THF solution (0.2 mL) of $Fe(acac)_3$ (2.1 mg, 6 mol%), bisphosphine (12 mol%), and *tert*-butyl 2-haloalkanoate (0.1 mmol) in a 5 mL microwave vial was added PhMgBr (0.50–1.0 M solution in THF, 1.5–2.0 equiv) slowly over 1–2 h using a syringe pump at 0 °C. After stirring at same temperature for 10 min, the resulting mixture was quenched with a 1.0 M aqueous solution (0.2 mL) of hydrochloric acid and extracted with diethyl ether (1 mL × 3). The organic layer was filtered through a plug of silica and concentrated in *vacuo*, the residue was purified by silica gel chromatography which was performed on prepacked silica-gel cartridges (SNAP Ultra; Biotage. hexane:EtOAc = 30:1).

4.2. tert-Butyl 2-chlorohept-6-enoate (**6a**)

Colorless liquid, 765.5 mg, 70% yield. ^{1}H NMR (400 MHz, $CDCl_3$) δ = 5.78 (ddt, J = 16.9, 10.2, 6.7 Hz, 1H), 5.05–4.98 (m, 2H), 4.16 (dd, J = 7.9, 6.1 Hz, 1H), 2.12–2.07 (m, 2H), 2.02–1.84 (m, 2H), 1.63–1.50 (m, 2H), 1.48 (s, 9H). ^{13}C NMR (150 MHz, $CDCl_3$) δ = 168.84, 137.89, 115.33, 82.55, 58.48, 34.44, 33.04, 27.96, 25.30. HRMS (ESI) calcd for $C_{11}H_{19}ClO_2Na$ $[M+Na]^+$ m/z = 241.0971; found 241.0969.

4.3. tert-Butyl 2-bromohept-6-enoate (**6b**)

Colorless liquid, 671.1 mg, 51% yield.^{1}H NMR (400 MHz, $CDCl_3$) δ = 5.78 (ddt, J = 16.9, 10.1, 6.7 Hz, 1H), 5.05–4.97 (m, 2H), 4.11 (t, J = 7.3 Hz, 1H), 2.12–1.90 (m, 4H), 1.64–1.43 (m, 2H), 1.48 (s, 9H). ^{13}C NMR (125 MHz, $CDCl_3$) δ = 168.97, 137.91, 115.39, 82.44, 47.81, 34.50, 33.05, 27.92, 26.65. HRMS (ESI) calcd for $C_{11}H_{19}BrO_2Na$ $[M+Na]^+$ m/z = 285.0466; found 285.0461.

4.4. Di-tert-butyl (E)-7-chlorooct-2-enedioate (**7a**)

Colorless liquid, 522.9 mg, 82% yield. ^{1}H NMR (400 MHz, $CDCl_3$) δ = 6.82 (dt, J = 15.6, 6.9 Hz, 1H), 5.76 (dt, J = 15.6, 1.6 Hz, 1H), 4.15 (dd, J = 7.9, 5.9 Hz, 1H), 2.25–2.18 (m, 2H), 2.03–1.86 (m, 2H), 1.71–1.53 (m, 2H), 1.49 (s, 9H), 1.48 (s, 9H). ^{13}C NMR (150 MHz, $CDCl_3$) δ = 168.64, 165.98, 146.57, 123.89, 82.77, 80.31, 58.28, 34.38, 31.31, 28.28, 27.97, 24.60. HRMS (ESI)calcd for $C_{16}H_{28}ClO_4$ $[M+H]^+$ m/z = 319.1676; found 319.1677.

4.5. Di-tert-butyl (E)-7-bromooct-2-enedioate (**7b**)

Colorless liquid, 581.3 mg, 80% yield. ^{1}H NMR (400 MHz, $CDCl_3$) δ = 6.80 (dt, J = 15.6, 6.9 Hz, 1H), 5.74 (dt, J = 15.6, 1.6 Hz, 1H), 4.09 (dd, J = 7.8, 6.8 Hz, 1H), 2.26–2.17 (m, 2H), 2.08–1.89 (m, 2H), 1.68–1.50 (m, 2H), 1.46 (s, 18H). ^{13}C NMR (125 MHz, $CDCl_3$) δ = 168.80, 166.02, 146.57, 123.93, 82.62, 80.37, 47.48, 34.43, 31.33, 28.31, 27.92, 25.94. HRMS (ESI) calcd for $C_{16}H_{28}BrO_4$ $[M+H]^+$ m/z = 363.1171; found 363.1165.

4.6. Di-tert-butyl (E)-7-iodooct-2-enedioate (**7c**)

Colorless liquid, 482.5 mg, 49% yield. ^{1}H NMR (600 MHz, $CDCl_3$) δ = 6.79 (dt, J = 15.6, 6.9 Hz, 1H), 5.73 (dt, J = 15.7, 1.6 Hz, 1H), 4.17 (t, J = 7.6 Hz, 1H), 2.22–2.14 (m, 2H), 1.97–1.88 (m, 2H), 1.61–1.53 (m, 2H), 1.46 (s, 9H), 1.44 (s, 9H). ^{13}C NMR (150 MHz, $CDCl_3$) δ = 170.28, 165.95, 146.56, 123.84, 82.12, 80.28, 35.61, 31.17, 28.27, 27.96, 27.72, 23.24. HRMS (ESI) calcd for $C_{16}H_{28}IO_4$ $[M+H]^+$ m/z = 411.1032; found 411.1020.

4.7. tert-Butyl 2-(2-(tert-butoxy)-2-oxo-1-phenylethyl) cyclopentanecarboxylate (**9**)

Colorless liquid, 2.9 mg, 8% yield of three diastereomers (dr = 2.3:16:1). Major diastereomer ^{1}H NMR (400 MHz, $CDCl_3$) δ = 7.29–7.27 (m, 4H), 7.25–7.20 (m, 1H), 3.49 (d, J = 11.8 Hz, 1H), 2.99 (td, J = 6.8, 3.3 Hz, 1H), 2.60 (tt, J = 11.9, 7.0 Hz, 1H), 1.93–1.87 (m, 2H), 1.82–1.74 (m, 1H), 1.52–1.48 (m, 10H), 1.45–1.41 (m, 1H), 1.39 (s, 9H), 1.23–1.18 (m, 1H). ^{13}C NMR (150 MHz, $CDCl_3$) δ = 175.14, 172.61, 139.86, 128.59, 127.98, 127.11, 80.64, 80.41, 54.75, 47.40, 47.23, 30.16, 28.93, 28.37, 28.11, 23.08. HRMS (ESI) calcd for $C_{22}H_{33}O_4$ $[M+H]^+$ m/z = 361.2379; found 361.2363.

4.8. tert-Butyl 2-(2-(tert-butoxy)-2-oxoethyl) cyclopentanecarboxylate (**10**)

Colorless liquid, 10.2 mg, 36% yield of one diastereomer. ^{1}H NMR (500 MHz, $CDCl_3$) δ = 2.79 (td, J = 7.6, 4.8 Hz, 1H), 2.46–2.42 (m, 1H), 2.39 (dd, J = 15.3, 6.5 Hz, 1H), 2.20 (dd, J = 15.3, 8.7 Hz, 1H), 1.89–1.78 (m, 4H), 1.60–1.56 (m, 1H), 1.50–1.46 (m, 1H), 1.45 (s, 18H). ^{13}C NMR (125 MHz, $CDCl_3$) δ = 174.68, 172.49, 80.31, 48.03, 40.01, 37.36, 31.18, 28.74, 28.35, 28.29, 23.69. HRMS (ESI) calcd for $C_{16}H_{29}O_4$ $[M+H]^+$ m/z = 285.2066; found 285.2056.

4.9. 7-Cyclopropylhept-6-enoic acid (**11**)

(5-carboxypentyl)triphenylphosphonium bromide [34] (1.98 g, 4.32 mmol) was suspended in THF (12 ml) at −20 °C. NaHMDS (2.0 M solution in THF, 4.32 mL, 8.64 mmol) was added dropwise into the suspension and further stirred for 20 min. The reaction mixture was then cooled to −78 °C and cyclopropanecarboxaldehyde (4.0 mmol) was added. After 18 h, the solvent was removed in *vacuo*. H_2O (60 ml) was added to the residue and extracted with diethyl ether (20 mL × 3). The diethyl ether layers were discarded while the H_2O layer was acidified to pH = 2 using HCl (1 M). The acidified aqueous layer was further extracted with ethyl acetate (20 mL × 3). The organic layers were combined, dried over sodium sulfate, filtered and concentrated to dryness. The

alkenoic acid was purified over silica gel using ethyl acetate:hexane: (1:1) to provide a colorless liquid in 356.7 mg, 53% (unoptimized) yield of inseparable (*Z*:*E* = 3.5:1) mixture. (*Z*) ^{1}H NMR (400 MHz, $CDCl_3$) δ = 10.15 (br s, 1H), 5.28 (dt, *J* = 10.7, 7.3 Hz, 1H), 4.78–4.73 (m, 1H), 2.38 (t, *J* = 7.5 Hz, 2H), 2.19 (qd, *J* = 7.4, 1.5 Hz, 2H), 1.73-1.65 (m, 2H), 1.57–1.40 (m, 3H), 0.74–0.70 (m, 2H), 0.33–0.29 (m, 2H). ^{13}C NMR (125 MHz, $CDCl_3$) δ = 179.53, 134.56, 127.56, 34.00, 29.31, 27.31, 24.44, 9.75, 6.99. HRMS (ESI) calcd for $C_{10}H_{15}O_2$ [M-H]$^-$ *m*/*z* = 167.1072; found 167.1065.

4.10. 2-Chloro-7-cyclopropylhept-6-enoic acid (**12**)

n-BuLi (1.47 mL, 2.5 M in hexane, 3.66 mmol) was added to a THF solution (3.5 mL) of diisopropylamine (0.61 mL, 4.33 mmol) at 0 °C, and the mixture was stirred at that temperature for 40 min, then cooled to −20 °C. After addition of *N*,N′-dimethylpropyleneurea (DMPU) (0.83 mL) and 7-cyclopropylhept-6-enoic acid **11** (*Z*:*E* = 3.5:1, 280 mg, 1.66 mmol) in THF (3.5 mL), the resulting yellow solution was stirred at −20 °C for 2 h. The reaction mixture was then cooled to −78 °C and a THF solution (3.5 mL) of CCl_4 (0.8 mL, 8.32 mmol) was added in a single aliquot, giving a black mixture. After stirring at −78 °C for 2 h and then at 0 °C for 1 h, NaCl (0.9 g) and 1 M aqueous solution of hydrochloric acid (5 mL) were added. The mixture was extracted with methyl *tert*-butyl ether (MTBE) (5 mL × 3) and the solvent was evaporated in *vacuo*. The residue was purified by silica-gel column chromatography (hexane:EtOAc:AcOH = 30:15:0.2) to furnish a yellow liquid, 316.3 mg, 94% yield (*Z*:*E* = 3.5:1). (*Z*) ^{1}H NMR (500 MHz, $CDCl_3$) δ = 5.27 (dt, *J* = 11.0, 7.0 Hz, 1H), 4.81–4.77 (m, 1H), 4.36 (dd, *J* = 8.1, 5.7 Hz, 1H), 2.25–2.21 (m, 2H), 2.14–2.08 (m, 1H), 2.07–1.96 (m, 1H), 1.64–1.56 (m, 2H), 1.56–1.49 (m, 1H), 0.75–0.71 (m, 2H), 0.34–0.31 (m, 2H). ^{13}C NMR (125 MHz, $CDCl_3$) δ = 174.71, 135.24, 126.76, 57.17, 34.41, 26.80, 26.13, 9.77, 7.04. HRMS (ESI) calcd for $C_{10}H_{14}O_2Cl$ [M-H]$^-$ *m*/*z* = 201.0682; found 201.0677.

4.11. tert-Butyl 2-chloro-7-cyclopropylhept-6-enoate (**13**)

Colorless liquid, 213.8 mg, 54% yield (*Z*:*E* = 3.5:1). (*Z*) ^{1}H NMR (600 MHz, $CDCl_3$) δ = 5.26 (dt, *J* = 10.8, 7.2 Hz, 1H), 4.78–4.75 (m, 1H), 4.17 (dd, *J* = 7.9, 6.1 Hz, 1H), 2.22–2.18 (m, 2H), 2.04–1.99 (m, 1H), 1.94–1.88 (m, 1H), 1.61–1.53 (m, 1H), 1.54–1.49 (m, 2H), 1.48 (s, 9H), 0.73–0.70 (m, 2H), 0.32–0.29 (m, 2H). ^{13}C NMR (150 MHz, $CDCl_3$) δ = 168.94, 134.99, 127.01, 82.52, 58.58, 34.57, 27.98, 26.89, 26.22, 9.73, 6.99. HRMS (ESI) calcd for $C_{14}H_{23}O_2ClNa$ [M+Na]$^+$ *m*/*z* = 281.1284; found 281.1286.

4.12. tert-Butyl anti-2-((E)-4-phenylbut-1-en-1-yl) cyclopentanecarboxylate (**15-anti-E**)

Colorless liquid, 18.1 mg, 60% yield. ^{1}H NMR (600 MHz, $CDCl_3$) δ = 7.30–7.26 (m, 2H), 7.19–7.17 (m, 3H), 5.50 (dtd, *J* = 15.3, 6.6, 0.9 Hz, 1H), 5.39 (ddt, *J* = 15.3, 7.7, 1.3 Hz, 1H), 2.67–2.64 (m, 2H), 2.63–2.58 (m, 1H), 2.33–2.28 (m, 3H), 1.90–1.80 (m, 3H), 1.69–1.65 (m, 2H), 1.43 (s, 9H), 1.37–1.33 (m, 1H). ^{13}C NMR (150 MHz, $CDCl_3$) δ = 175.46, 142.24, 133.49, 129.31, 128.59, 128.38, 125.87, 79.95, 51.79, 48.05, 36.25, 34.60, 33.41, 29.93, 28.34, 24.52. HRMS (ESI) calcd for $C_{20}H_{29}O_2$ [M+H]$^+$ *m*/*z* = 301.2167; found 301.2167.

4.13. tert-Butyl anti-2-((Z)-4-phenylbut-1-en-1-yl) cyclopentanecarboxylate (**15-anti-Z**)

Colorless liquid, 7.5 mg, 25% yield. ^{1}H NMR (600 MHz, $CDCl_3$) δ = 7.28–7.26 (m, 2H), 7.20–7.17 (m, 3H), 5.39 (dt, *J* = 10.8, 7.8 Hz, 1H), 5.27 (ddt, *J* = 11.0, 9.6, 1.5 Hz, 1H), 2.98–2.92 (m, 1H), 2.71–2.66 (m, 1H), 2.63–2.58 (m, 1H), 2.45–2.33 (m, 2H), 2.30 (q, *J* = 8.4 Hz, 1H), 1.95–1.89 (m, 1H), 1.84–1.78 (m, 1H), 1.76–1.64 (m, 3H), 1.41 (s, 9H), 1.28–1.23 (m, 1H). ^{13}C NMR (125 MHz, $CDCl_3$) δ = 175.42, 142.18, 133.72, 128.99, 128.64, 128.37, 125.88, 79.96, 52.46, 42.92, 36.36, 33.92, 30.25, 29.56, 28.29, 24.82. HRMS (ESI) calcd for $C_{20}H_{29}O_2$ [M+H]$^+$ *m*/*z* = 301.2167; found 301.2175.

Acknowledgments

We acknowledge the National Science Foundation (CAREER, 1751568) and the University of Maryland College Park (start-up funds) for financial support. We thank the University of Maryland College Park (UMD) and the Maryland Advance Research Computing for access to Deepthought2 and BlueCrab computational clusters, respectively. We acknowledge the XSEDE (CHE160082 and CHE160053) for supercomputer access. We also acknowledge the Analytical NMR Service & Research Center (UMD) for NMR service/help provided by Dr. Yinde Wang and Dr. Fu Chen. We also thank Dr. Yue Li (UMD) for help with the HRMS.

Appendix A. Supplementary data

Supplementary data to this article can be found online at https://doi.org/10.1016/j.tet.2018.11.043.

References

[1] (a) C. Torborg, M. Beller, Adv. Synth. Catal. 351 (2009) 3027–3043;
(b) A. Suzuki, Angew Chem. Int. Ed. 50 (2011) 6722–6737;
(c) F.S. Han, Chem. Soc. Rev. 42 (2013) 5270–5298;
(d) D. Hass, J.M. Hammann, R. Greiner, P. Knochel, ACS Catal. 6 (2016) 1540–1552.
[2] (a) T.L. Mako, J.A. Byers, Inorg. Chem. Front. 3 (2016) 766–790;
(b) C. Cassani, G. Bergonzini, C.-J. Wallentin, ACS Catal. 6 (2016) 1640–1648.
[3] (a) T. Hatakeyama, Y. Kondo, Y. Fujiwara, H. Takaya, S. Ito, E. Nakamura, M. Nakamura, Chem. Commun. (2009) 1216–1218;
(b) T. Hatakeyama, Y. Fujiwara, Y. Okada, T. Itoh, T. Hashimoto, S. Kawamura, K. Ogata, H. Takaya, M. Nakamura, Chem. Lett. 40 (2011) 1030–1032;
(c) T. Hatakeyama, T. Hashimoto, K.K.A.D.S. Kathriarachchi, T. Zenmyo, H. Seike, M. Nakamura, Angew Chem. Int. Ed. 51 (2012) 8834–8837;
(d) T. Hatakeyama, T. Hashimoto, Y. Kondo, Y. Fujiwara, H. Seike, H. Takaya, Y. Tamada, T. Ono, M. Nakamura, J. Am. Chem. Soc. 132 (2010) 10674–10676;
(e) T. Hatakeyama, Y. Okada, Y. Yoshimoto, M. Nakamura, Angew Chem. Int. Ed. 50 (2011) 10973–10976;
(f) S. Kawamura, M. Nakamura, Chem. Lett. 42 (2013) 183–185;
(g) N. Nakagawa, T. Hatakeyama, M. Nakamura, Chem. Lett. 44 (2015) 486–488.
[4] (a) R.B. Bedford, M. Huwe, M.C. Wilkinson, Chem. Commun. (2009) 600–602;
(b) C.J. Adams, R.B. Bedford, E. Carter, N.J. Gower, M.F. Haddow, J.N. Harvey, M. Huwe, M.A. Cartes, S.M. Mansell, C. Mendoza, D.M. Murphy, E.C. Neeve, J. Nunn, J. Am. Chem. Soc. 134 (2012) 10333–10336;
(c) R.B. Bedford, E. Carter, P.M. Cogswell, N.J. Gower, M.F. Haddow, J.N. Harvey, D.M. Murphy, E.C. Neeve, J. Nunn, Angew Chem. Int. Ed. 52 (2013) 1285–1288;
(d) R.B. Bedford, P.B. Brenner, E. Carter, T.W. Carvell, P.M. Cogswell, T. Gallagher, J.N. Harvey, D.M. Murphy, E.C. Neeve, J. Nunn, D.R. Pye, Chem. Eur. J 20 (2014) 7935–7938.
[5] K.G. Dongol, H. Koh, M. Sau, C.L.L. Chai, Adv. Synth. Catal. 349 (2007) 1015–1018.
[6] C.-L. Sun, H. Krause, A. Fürstner, Adv. Synth. Catal. 356 (2014) 1281–1291.
[7] (a) F. Toriyama, J. Cornella, L. Wimmer, T.-G. Chen, D.D. Dixon, G. Creech, P.S. Baran, J. Am. Chem. Soc. 138 (2016) 11132–11135;
(b) J.T. Edwards, R.R. Merchant, K.S. McClymont, K.W. Knouse, T. Qin, L.R. Malins, B. Vokits, S.A. Shaw, D.-H. Bao, F.-L. Wei, T. Zhou, M.D. Eastgate, P.S. Baran, Nature 545 (2017) 213–218.
[8] For recent studies, see: (a) S.L. Daifuku, M.H. Al-Afyouni, B.E.R. Snyder, J.L. Kneebone, M.L. Neidig, J. Am. Chem. Soc. 136 (2014) 9132–9143;
(b) S.L. Daifuku, J.L. Kneebone, B.E.R. Snyder, M.L. Neidig, J. Am. Chem. Soc. 137 (2015) 11432–11444;
(c) J.L. Kneebone, W.B. Brennessel, M.L. Neidig, J. Am. Chem. Soc. 139 (2017) 6988–7003.
[9] M. Jin, L. Adak, M. Nakamura, J. Am. Chem. Soc. 137 (2015) 7128–7134.
[10] (a) M. Nakamura, A. Hirai, E. Nakamura, J. Am. Chem. Soc. 122 (2000) 978–979;
(b) H. Egami, K. Matsumoto, Oguma, T. Kunisu, T. Katsuki, J. Am. Chem. Soc. 132 (2010) 13633.
[11] A.H. Cherney, N.T. Kadunce, S.E. Reisman, Chem. Rev. 115 (2015) 9587–9652.
[12] A.K. Sharma, W.M.C. Sameera, M. Jin, L. Adak, C. Okuzono, T. Iwamoto, M. Kato,

M. Nakamura, K. Morokuma, J. Am. Chem. Soc. 139 (2017) 16117–16125.
[13] L. Wes, J. Zhou, O. Gutierrez, J. Am. Chem. Soc. 139 (2017) 16126–16133.
[14] (a) J. Choi, P. Martin-Gago, G.C. Fu, J. Am. Chem. Soc. 136 (2014) 12161–12165;
(b) S. Biswas, D.J. Weix, J. Am. Chem. Soc. 135 (2013) 16192–16197.
[15] M.J. Frisch, G.W. Trucks, H.B. Schlegel, G.E. Scuseria, M.A. Robb, J.R. Cheeseman, G. Scalmani, V. Barone, B. Mennucci, G.A. Petersson, H. Nakatsuji, M. Caricato, X. Li, H.P. Hratchian, A.F. Izmaylov, J. Bloino, G. Zheng, J.L. Sonnenberg, M. Hada, M. Ehara, K. Toyota, R. Fukuda, J. Hasegawa, M. Ishida, T. Nakajima, Y. Honda, O. Kitao, H. Nakai, T. Vreven, J.A. Montgomery Jr., J.E. Peralta, F. Ogliaro, M. Bearpark, J.J. Heyd, E. Brothers, K.N. Kudin, V.N. Staroverov, R. Kobayashi, J. Normand, K. Raghavachari, A. Rendell, J.C. Burant, S.S. Iyengar, J. Tomasi, M. Cossi, N. Rega, J.M. Millam, M. Klene, J.E. Knox, J.B. Cross, V. Bakken, C. Adamo, J. Jaramillo, R. Gomperts, R.E. Stratmann, O. Yazyev, A.J. Austin, R. Cammi, C. Pomelli, J.W. Ochterski, R.L. Martin, K. Morokuma, V.G. Zakrzewski, G.A. Voth, P. Salvador, J.J. Dannenberg, S. Dapprich, A.D. Daniels, Ö. Farkas, J.B. Foresman, J.V. Ortiz, J. Cioslowski, D.J. Fox, Gaussian 09, Revision E.01, Gaussian, Inc, Wallingford CT, 2009.
[16] (a) F. Neese, The ORCA program system, Wiley Interdiscip. Rev. Comput. Mol. Sci. 2 (2012) 73–78;
(b) C. Riplinger, B. Sandhoefer, A. Hansen, F. Neese, J. Chem. Phys. 139 (2013) 134101–134113.
[17] M. Newcomb, Radical kinetics and clocks, in: C. Chatgilialoglu, A. Studer (Eds.), Encyclopedia of Radicals in Chemistry, Biology, and Materials, Wiley, Hoboken, NJ, 2012.
[18] Preliminary results have shown that modest enantioselectivity (67: 33 *er*) in the tandem radical cyclization-arylation reaction.
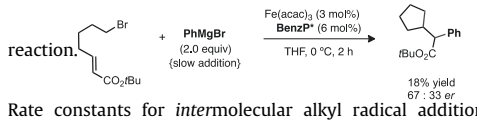

[19] Rate constants for *inter*molecular alkyl radical addition onto substituted olefins has shown a ca. 100-fold rate increase in ester-substituted olefins compared with alkyl substituted olefins. Reference 17.
[20] X. Guan, D.L. Phillips, D. Yang, J. Org. Chem. 71 (2006) 1984–1988.
[21] Notably, the reaction without iron and ligand, at 90% conversion, underwent decomposition without formation of arylated products.
[22] F. Alonso, I.P. Beletskaya, M. Yus, Chem. Rev. 102 (2002) 4009–4091.
[23] The reaction without iron and ligand, at 89% conversion, underwent decomposition without formation of arylated products.
[24] Interestingly, the reaction without iron and ligand, at 100% conversion, provided 72% yield of product **10** (*dr* = 1.6:1) without formation of cross-coupling products.
[25] M. Jin, M. Nakamura, Chem. Lett. 40 (2011) 1012–1014.
[26] We only considered the quartet spin states for this arylation process. Previously (ref. 13), we demonstrated arylation via double and sextet spin states was much higher in energy.
[27] The lowest energy barrier (enthalpy and free energy in parenthesis and brackets, respectively) for radical cyclization of: **2b•** is 8.4 (7.6) [10.7] (UB3LYP/6-31G(d) method) 4.7 (3.9) [7.0] ((U)DLPNO-CCSD(T)/def2-TZVPP//UB3LYP/6-31G(d) method); **8•** is 7.2 (6.5) [10.1] (UB3LYP/6-31G(d) method) 4.4 (3.8) [7.3] ((U)DLPNO-CCSD(T)/def2-TZVPP//UB3LYP/6-31G(d) method). See Supporting information for full diagram.
[28] (a) J.T. Barry, D.J. Berg, D.R. Tyler, J. Am. Chem. Soc. 138 (2016) 9389–9392;
(b) J.T. Barry, D.J. Berg, D.R. Tyler, J. Am. Chem. Soc. 139 (2017) 14399–14405.
[29] L.A. Paquette, Synlett (2001) 1–12.
[30] H. Fisher, Chem. Rev. 101 (2001) 3581–3610.
[31] A. Padwa, L.S. Beall, T.M. Heidelbaugh, B. Liu, S.M. Sheehan, J. Org. Chem. 65 (2000) 2684–2695.
[32] F.C. Bargiggia, W.V. Murray, J. Org. Chem. 70 (2005) 9636–9639.
[33] K.P. McGrath, A.,H. Hoveyda, Angew Chem. Int. Ed. 53 (2014) 1910–1914.
[34] C.K. Tan, L. Zhou, Y. Yeung, Org. Lett. 13 (2011) 2738–2741.